River Flow 2010 - Dittrich, Koll, Aberle & Geisenhainer (eds) - © 2010 Bundesanstalt für Wasserbau ISBN 978-3-939230-00-7

# Shear Stress Measurements over Smooth and Rough Channel Beds

E. Carvalho, R. Maia & M. F. Proença
*Departamento de Engenharia Civil, Faculdade de Engenharia da Universidade do Porto, Porto, Portugal*

ABSTRACT: In fluvial hydraulics the knowledge of the fluid-bed interaction is an important factor to study the stability of fluvial beds. One way to characterize that interaction is through the evaluation of the shear stress at the wall. Indirect methods are often used to evaluate the shear stress. However, the use of those methods such as the velocity Log-Law, is not always straightforward: for example, in some flows it has to be proved that the law of the wall definition still holds and its parameters determined. In this paper an experimental study of the shear stress developed at a rectangular channel bed is presented and different methods are compared. Measurements were carried out in an open channel for different flow conditions, defined by a Reynolds number range from $1\times10^4$ to $5\times10^4$ and with Froude numbers between 0.2 and 1.7. Flows were established over smooth (perspex plate and sandpaper) and rough beds (uniform glass spheres). Direct measurements of the shear stress were obtained by means of an optical Doppler based shear stress probe. Indirect methods' velocity profiles characterization was made by means of two-component Laser Doppler Anemometer measurements. Obtained results are compared and the limitations and advantages of each method are discussed.

*Keywords: Shear Stress Measurements, Shear Stress Probe, Rough beds, Smooth beds*

## 1 INTRODUCTION

In Fluvial Hydraulics the fluid-bed interaction is an important parameter to the study of the stability of fluvial beds. This interaction can be characterized through the evaluation of the shear stress at the wall which is a function of such variables as the roughness of the bed and the type of the flow.

The present study is focused on the determination of the shear stress developed on different channel bottoms which is a part of a research work on the beginning of sediment motion. For that purpose, different flow conditions as well as different bed roughness have been considered. Several methods were used and the obtained results are compared and analyzed.

## 2 SHEAR STRESS MEASUREMENTS

The shear stress definition at the wall is given by:

$$\tau_w = \mu \left.\frac{\partial u}{\partial y}\right|_w \qquad (1)$$

where $\tau_w$ = shear stress at the wall, $\mu$ = dynamic fluid viscosity and $\partial u/\partial y|_w$ = velocity gradient at the wall.

The fact that it depends on the fluid's velocity gradient measured at the wall leads to major difficulties when an accurate measure is needed. In order to evaluate the shear stress value two major classes of methods can be used: indirect and direct methods. Indirect methods are often used as an expedite way for shear stress evaluation. In general these methods are based on the determination of the shear velocity, $u_*$, which is related with the shear stress through the following expression:

$$\tau = \rho\, u_*^{\,2}, \qquad (2)$$

where $\rho$ = fluid density.

Direct methods that are able to measure directly the shear stress value can be of different types: floating-elements balances (Acharya et al. (1985)), thermal techniques or optical techniques, like the shear stress probe used in the scope of this paper (Tavoularis (2005)).

The shear stress is also dependent of the type of wall considered: smooth or rough. The wall

roughness can be characterized by the roughness Reynolds number, $Re_*$, given by:

$$\mathrm{Re}_* = \frac{k_s u_*}{\nu} \tag{3}$$

where $k_S$ = equivalent roughness and $\nu$ = kinetic viscosity.

A flow is said to be smooth if $Re_*<5$, corresponding to all the roughness elements being inside the viscous sub-layer. A transitional flow occurs when $5<Re_*<70$ and if $Re_*>70$ the flow is said to be rough. For this case the viscous sub-layer is so thin that the roughness elements penetrate the logarithmic layer (Graf & Altinakar (1998)).

The magnitude of the wall roughness will affect also the choice of the measuring method to use.

### 2.1 *Shear Stress Evaluation over a Smooth Bed*

#### 2.1.1 *Doppler shear stress probe*

The working principle of the shear stress probe is based on the Doppler effect. The probe is connected to a laser light source through a fiber optic cable. On the probe's head an optical grid generates a fringe pattern that will form the control volume. This control volume is located at a very small distance from the wall, usually in the range of micrometers, in order to be inside the viscous sub-layer, where the velocity profile presents a constant gradient.

When flow seeding particles cross the control volume they scatter light that will be collected by a photodetector placed near the probe emitter (Figure 1). It can be demonstrated that the Doppler frequency of the particles that cross the imaged region is proportional to the velocity gradient at the wall (Gharib et al. (2001)):

$$f_D = \alpha \left.\frac{\partial u}{\partial y}\right|_w \tag{4}$$

where $f_D$ = Doppler frequency, $\alpha$ = constant and $\partial u/\partial y|_w$ = the velocity gradient at the wall. The shear stress at the wall can therefore be evaluated as:

$$\tau_w = \mu \left.\frac{\partial u}{\partial y}\right|_w = \mu \beta f_D \tag{5}$$

where $\beta$ = probe's constant that is a function of the fringes' divergence and $f_D$ = Doppler frequency.

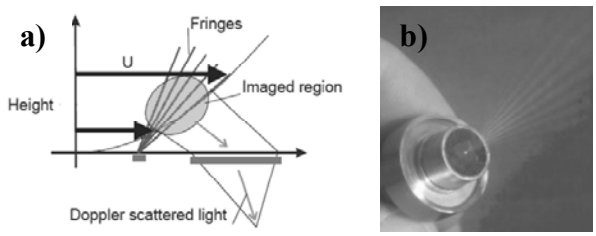


Figure 1. Shear stress probe: a) working principle; b) fringe pattern (adapted from Gharib et al. (2001)).

The shear stress probe has the advantages of a common LDA: non-intrusive since it is flush mounted on the channel's bottom, requires no calibration and has a linear response. It also shares the same disadvantages of a common LDA: seeding is needed and measured data has a stochastic sampling rate. One limitation to the use of this technique is imposed by the viscous sub-layer dimensions that in principle limit the use of this method to hydraulically smooth flows.

#### 2.1.2 *The bed-slope method*

For uniform flow the shear velocity can be easily evaluated from the bed slope value, $S$, and flow section characteristics (Graf & Altinakar (1998), Rowinski et al. (2005)):

$$\tau = \gamma R_h S \tag{6}$$

where $\gamma$ = specific weight, $R_h$ = hydraulic radius and $S$ = channel slope.

This method can also be applied to rough beds.

#### 2.1.3 *The Logarithmic Law method*

The Logarithmic Law (Log-Law) is commonly used to evaluate the shear velocity by fitting to the experimental velocity profile data the following equation:

$$u^+ = \frac{1}{k}\ln\left(y^+\right) + B \tag{7}$$

where $u^+ = u/u_*$ (where $u$ is the mean velocity horizontal component), $k$ = von Kármán constant (considered $k = 0.41$), $y^+ = yu_*/\nu$ (where $y$ = vertical coordinate and $\nu$ = the kinetic viscosity) and $B$ = constant, usually $B$=5 (Graf & Altinakar (1998)).

#### 2.1.4 *Reynolds Stress method*

The total shear stress distribution, in a full developed and two-dimensional flow, is given by (Tennekes & Lumley (1972))

$$\tau = -\overline{u'v'} + \nu\frac{du}{dy} = u_*^2\left(1 - \frac{y}{h}\right) \tag{10}$$

where $\overline{u'v'}$ = Reynolds Stress, $\nu\, du/dy$ = viscous stress and $h$ = flow depth. Neglecting the viscous stress equation (10) reduces to

$$-u'v' = u_*^2\left(1-\frac{y}{h}\right) \tag{11}$$

from which is possible to determine the shear velocity by measuring the Reynolds stress profiles. This method is also valid for hydraulically rough beds with the introduction of a theoretical bottom as described in the following section.

### 2.2 *Shear Stress Evaluation over a Rough Bed*

As stated before the bed slope method (2.1.2) and the Reynolds stress method (2.1.4) can also be applied on rough beds.

#### 2.2.1 *Logarithmic Law method*

When considering rough beds there will be an additional parameter to account for. If for the smooth bed there is no problem with the determination of the zero bed level, the same can not be said about a rough bed. In this last case, despite the big amount of existent studies on the subject, there is not a consensus about the position of the origin. For the rough beds case it is often considered a virtual origin which according to Nezu & Nakagawa (1993) should be located at a certain distance bellow the top of the spheres, here designated by displacement height $\Delta y$, whose values is $0<\Delta y<k_S$ (Figure 2).

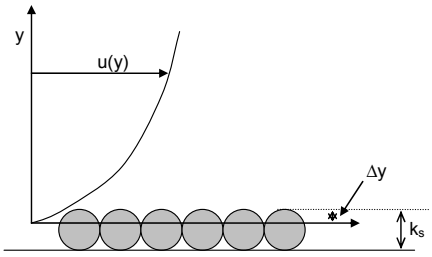

Figure 2. Scheme of the flow over a rough bed.

Different values for this distance are presented in literature. Bayazit (1976) found $\Delta y=0.35k_S$ based on experiments with 23mm diameter hemispheres. Grass (1971) determined $\Delta y=0.18k_S$ with 9mm rounded pebbles experiments and Graf & Altinakar (1998) present the general value $\Delta y=0.2k_S$.

The displacement height can be evaluated when calculating the shear velocity trough different methods.

In rough beds the Log-Law can be formulated as:

$$u^+ = \frac{1}{k}\ln\frac{y}{k_S} + C \tag{12}$$

where $k_S$ = equivalent roughness, in this study considered equal to the spheres diameter, $D$, and $C$ = constant, typically used as $C$=8.5 (Bayazit (1976), Biron et al. (2004)).
The application of the least square fitting of the equation (12) to the experimental velocity data allows the simultaneous evaluation of the shear velocity and of the displacement height.

#### 2.2.2 *Total Shear Stress method*

In rough beds the spatial variability in the time-averaged flow characteristics can be important and a form-induced stress should be considered.

Using the double averaging methodology (Pokrajac et al. (2006)), the total shear stress above the roughness crests is given by:

$$\tau = \rho\left(\nu\frac{du}{dy} - \overline{u'v'} - \widetilde{u}\widetilde{v}\right) \tag{13}$$

where $\widetilde{u}\widetilde{v}$ = form-induced stress.

Above the crests of the roughness elements the total shear stress profiles are linear. In this case, and neglecting the viscous stress, the bed shear stress can be evaluated from the intersection of the total shear stress profile with the theoretical bottom level.

The flow depth measured from the theoretical bottom can be evaluated as (Ferreira et al. (2008)):

$$h_* = h - \delta(1-\phi_m) \tag{14}$$

where $h_*$ = flow depth corresponding to that theoretical bottom level, $h$ = flow depth measured from the channel bottom, $\delta$ = distance between the highest crests and the lowest troughs and $\phi_m$ = volume between the plane of the troughs and the plane of the crests (mean void fraction of the bed surface).

## 3 EXPERIMENTAL SETUP

### 3.1 *The Water Channel*

The measurements were carried out in the small open channel of the Hydraulics Laboratory at Faculty of Engineering of Porto University which is included into the recirculation water system of the Laboratory. The channel is represented in Figure 3, has a constant rectangular section of 0.40m width and 0.60m height, is 17m long and is supported on a pivoting support allowing the adjustment of the bottom slope. The channel glass walls allow visual access to the test section enabling also the use of Laser Doppler Anemometry technique in both forward and backscatter modes.

Flow rate control is achieved by means of an upstream valve located at the feeding pipe, as shown in Figure 3 a) and measured by an electro-magnetic flowmeter (Figure 3 b)). A sluice gate located at the downstream channel section allows the control of the flow depth (Figure 3 d)).

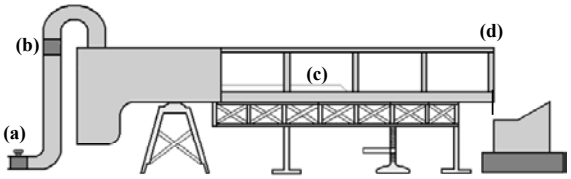


Figure 3. Open Channel scheme where: (a) valve, (b) flow meter, (c) double bottom and (d) sluice gate.

A double bottom of 0.4m width and 8m length was mounted in the channel allowing, by replacement of some of its stretches, the test of different bottom roughness (Figure 4). The different types of roughness tested were: a) smooth perspex plate b) 0.262 mm sandpaper and c) 4mm glass spheres. The correspondent roughness elements (Figure 4 c)) were placed over a plate of 1m length and 0.4m wide, in such a way that the roughness crest levels match top of the remaining double bottom level plates. The rough test section is placed 6.5m from the beginning of the double bottom assuring the fully developed boundary layer as verified by complementary velocity profiles measurements.

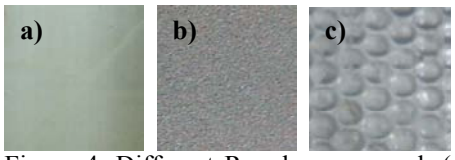


Figure 4. Different Roughnesses used: (a) smooth perspex plate, (b) Sandpaper (c) Uniform glass spheres.

For the uniform glass spheres roughness (Figure 4 c)) a triangular arrangement was considered as shown in Figure 5.

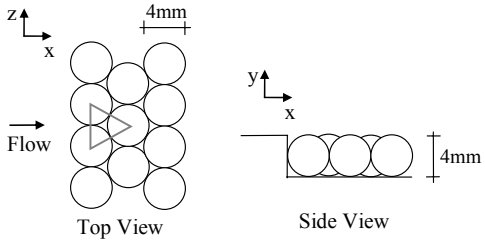


Figure 5. Uniform spheres bed arrangement.

### 3.2 *Shear Stress Probe*

The Measurement Science Enterprise® shear stress probe used is presented on Figure 1 b). In Table 1 the main characteristics of the shear stress probe are presented.

Table 1. Shear Stress Probe Characteristics

| Parameter | Value |
|---|---|
| Fringe divergence | 0.0845μm |
| Control Volume Position above bed | 172.9μm |

### 3.3 *Laser Doppler Anemometer*

In order to apply the indirect methods accurate velocity measurements were required. Those measurements have been carried out using a two component fiber optic Laser Doppler Anemometer (LDA) from DANTEC, working in forward-scatter mode.

The LDA technique is nowadays an established and mature technique. A detailed description of this technique can be found on Durst et al. (1981).

The velocity measurements were carried out using a two-component LDA in order to measure also the Reynolds stress. The acquired signal was processed by a Burst Spectrum Analyzer from DANTEC. The main characteristics of the Laser Doppler Anemometer are shown in Table 2.

A 400mW Argon-Ion Laser source operating in multi-mode was used.

Table 2. Laser Doppler Anemometer Characteristics

| | LDA1 | LDA2 |
|---|---|---|
| Wavelength | 514.5nm | 488nm |
| Dimensions of the control volume | | |
| Major axis | 2.825mm | 2.679mm |
| Minor axis | 0.08189mm | 0.07767mm |

### 3.4 *Experimental Conditions*

Two sets of experiments were carried out for different flow conditions and the different bed roughness presented in section 3.1. Two different channel slopes (S) were considered: 0% for smooth bed and 1.3% for uniform spheres bed, a condition to be used on the referred research work on the beginning of sediment motion. For S=0% the flow is subcritical, however the flow can be considered as uniform over the test section, since the control section is far away from the test section

The tested flow conditions are summarized in Tables 3 to 5. The flow variables used to define the different flow conditions are the flow rate, $Q$, the flow depth, $h$, the Reynolds number, Re, defined by $\mathrm{Re}=UR_h/\nu$ ($U$ is the mean velocity, $R_h$ is the hydraulic radius and $\nu$ is the kinetic viscosity), and Froude number, Fr, evaluated as $\mathrm{Fr}=U/(gh)^{0.5}$ ($g$ is the gravitational acceleration). Each condition designation is defined by the channel slope ($S$=0% (*S0*) or $S$=1.3% (*S1.3*)) and by flow condition reference number (*Ci*).

In Table 3 the flow conditions and bed characteristics tested are shown.

Table 3. Tested conditions

| Flow Regime | Subcritical | Supercritical |
|---|---|---|
| Bed Roughness | Perspex plate Sandpaper | Glass spheres |
| Channel Slope | 0% | 1.3% |

Table 4 presents the mean flow parameters for the perspex bed (identical for sand paper bed), while Table 5 resumes the mean flow parameters for the uniform spheres bed.

Table 4. Tested mean flow conditions over perspex bed (S=0%)

| Flow Condition | $Q$ [L/s] | $U$ [m/s] | $h$ [mm] | Re [-] | Fr [-] |
|---|---|---|---|---|---|
| S0C1 | 5 | 0.223 | 56 | $9.8x10^3$ | 0.09 |
| S0C2 | 7.5 | 0.313 | 60 | $1.3x10^4$ | 0.17 |
| S0C3 | 15 | 0.421 | 89 | $2.4 x10^4$ | 0.20 |
| S0C4 | 20 | 0.485 | 103 | $3.3 x10^4$ | 0.23 |
| S0C5 | 12 | 0.300 | 100 | $2.0 x10^4$ | 0.09 |
| S0C6 | 20 | 0.321 | 156 | $2.8 x10^4$ | 0.07 |
| S0C7 | 30 | 0.419 | 179 | $3.9 x10^4$ | 0.10 |

Table 5. Tested mean flow conditions over uniform spheres bed (S=1.3%)

| Flow Condition | $Q$ [L/s] | $U$ [m/s] | $h$ [mm] | Re [-] | Fr [-] |
|---|---|---|---|---|---|
| S1.3C1 | 5 | 0.614 | 20.5 | $1.1x10^4$ | 1.37 |
| S1.3C2 | 7.5 | 0.763 | 24.5 | $1.8x10^4$ | 1.56 |
| S1.3C3 | 8.75 | 0.819 | 26.8 | $2.0x10^4$ | 1.60 |
| S1.3C4 | 10 | 0.840 | 29.8 | $2.1x10^4$ | 1.55 |
| S1.3C5 | 15 | 1.019 | 37.0 | $3.1x10^4$ | 1.69 |
| S1.3C6 | 20 | 1.126 | 44.5 | $4.2x10^4$ | 1.70 |

## 4 EXPERIMENTAL RESULTS

### 4.1 *Mean Velocity Profiles*

For the perspex and sandpaper cases only one velocity profile was measured for each flow condition, since that was enough to determine the shear stress. However, for the bed made of spheres five velocity profiles (Pi) have been measured around a particle in the positions indicated on Figure 6. These measurements are required to allow the use of the total stress method where the spatial variability of the flow characteristics must be taken into account as shown in section 2.2.2.

In Figure 7 the horizontal velocity component profiles are shown for the referred three different bed roughnesses. For the case of uniform glass spheres only the velocity profiles measured on the crest of the spheres are presented (P1 in Figure 6). Mean velocity values and vertical coordinates have been normalized by the maximum vertical velocity component, $U_\infty$, and correspondent vertical coordinate, $y_{max}$, respectively.

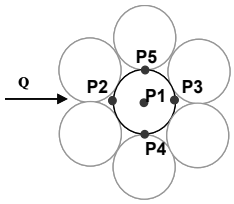


Figure 6. Uniform spheres bed arrangement and measuring points.

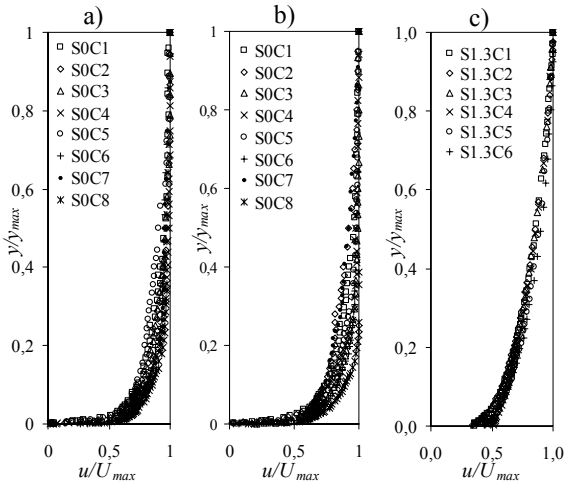


Figure 7. Horizontal component of the mean velocity for the different bed roughness: a) perspex plate; b) sandpaper; c) uniform glass spheres (take $U_{max}=U_\infty$).

As an example, five horizontal velocity component profiles (measured according to the positions of Figure 6) are presented in Figure 8 for one of the tested flow conditions. Figure 8 b) shows that the most significant differences between the depicted velocity profiles occur mainly near the wall, probably due to the positioning of the laser control volume over a spherical cap.

The geometry of the bottom and the LDA's laser beams configuration used only made possible the measurement of velocity's vertical component starting 4mm above the spheres' crest. The correspondent obtained results have shown mean local velocity values to be about zero.

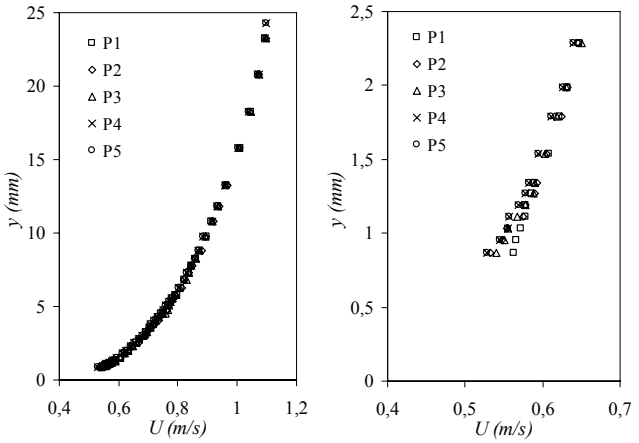


Figure 8. (a) Horizontal mean velocity profiles for the flow condition S1.3C3. (b) zoom for values near the wall.

## 4.2 *Shear Stress Evaluation*

### 4.2.1 *Perspex and Sandpaper beds*

To measure the shear-stress on the perspex plate and on the sandpaper the Shear Stress Probe and the Log-Law method described in 2.1.1 and 2.1.3 respectively, were used. The values of the measured shear velocity are shown in Table 6.

Table 6. Measured shear velocity values, $u_*$ [m/s]: perspex and sandpaper.

| Flow | $u_*$ [m/s] Perspex | | $u_*$ [m/s] SandPaper | |
|---|---|---|---|---|
| Condition | Log-Law | Probe | Log-Law | Probe |
| S0C1 | 0.0124 | 0.0121 | 0.0116 | 0.0102 |
| S0C2 | 0.0178 | 0.0181 | 0.0165 | 0.0171 |
| S0C3 | 0.0208 | 0.0207 | 0.0205 | 0.0196 |
| S0C4 | 0.0240 | 0.0239 | 0.0233 | 0.0234 |
| S0C5 | 0.0161 | 0.0155 | 0.0158 | 0.0151 |
| S0C6 | 0.0155 | 0.0160 | 0.0166 | - |
| S0C7 | 0.0197 | 0.0196 | 0.0185 | 0.0183 |

These data points are plotted in Figure 9 and the relation between the direct measurements and the ones obtained through the Log-Law method is shown. It is possible to see that there is a good agreement between the results of the two methods.

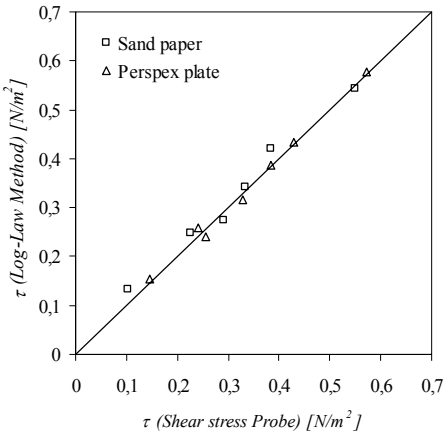


Figure 9. Comparison of shear stress values obtained with the shear stress probe and the Log-Law method for different conditions of hydraulic smooth flows.

The mean velocity profiles normalized with the shear velocity obtained from the Log-Law method are presented in figure 10.

Using the values of the shear velocity presented on Table 6 and the diameter of the sandpaper roughness elements the roughness Reynolds number (equation (3)) have been evaluated and showed to be in the range of the ones correspondent to smooth flows according to Graf and Altinakar (1998).

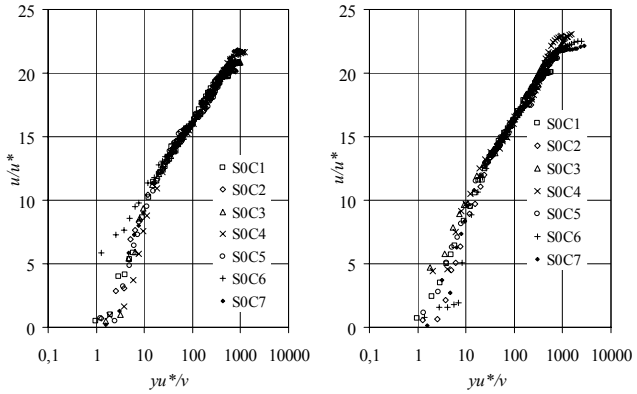


Figure 10. Mean velocity profiles normalized with $u^*$: (a) perspex plate; (b) Sandpaper.

### 4.2.2 *Uniform spheres bed*

For the flow over a bed of uniform spheres the shear velocity was evaluated using the bed-slope method (2.1.2), the Reynolds Stress method (2.1.4), the Log-Law method (2.2.1) and the total stress method (2.2.2) as described in Section 2. Some preliminary tests with the shear stress probe have shown that the results were inconsistent, due to the fact that the viscous sub-layer was probably too thin. Therefore, the shear stress probe was not used in this case.

The application of the Log-Law and the total stress methods allowed the simultaneous calculation of the displacement height as referred in section 2.2. Table 7 presents the shear velocity values obtained with the referred methods as well as the displacement height evaluated from the Log-Law method. It must be pointed out that in the case of using the total shear stress method all the flow conditions have the same displacement heights due to the uniformity of the bed roughness.

Table 7. Measured shear velocity values, $u_*$ [m/s] and displacement height normalized with the roughness diameter, $\Delta y/k_S$ [-], for uniform bed spheres.

| Flow | $\Delta y/k_S$ | $u_*$ [m/s] | | | |
|---|---|---|---|---|---|
| Condition | Log-Law | Log-Law | $\gamma R_h S$ | u'v' | $\tau_{total}$ |
| S1.3C1 | 0.15 | 0.0679 | 0.0495 | 0.0442 | 0.0443 |
| S1.3C2 | 0.19 | 0.0732 | 0.0535 | 0.0602 | 0.0564 |
| S1.3C3 | 0.20 | 0.0767 | 0.0556 | 0.0616 | 0.0613 |
| S1.3C4 | 0.44 | 0.0822 | 0.0582 | 0.0664 | 0.0704 |
| S1.3C5 | 0.47 | 0.0910 | 0.0637 | 0.0710 | 0.0723 |
| S1.3C6 | 0.46 | 0.0895 | 0.0686 | 0.0720 | 0.0692 |

Analyzing the obtained results it is possible to conclude that shear velocity values obtained from Log-Law are around 20% to 30% higher than the ones obtained through the other methods. This can be due to the fact that it was not always possible to identify the limits of the logarithmic region on the velocity profile. In what concerns the displacement height obtained from the Log-Law method it is possible to observe two groups of values

around 0.2 and 0.45. In the case of total stress method a constant value of 0.20 was obtained.

Using the values presented on Table 7 along with the particles' diameter the roughness Reynolds number (equation (3)) has been evaluated. All values were greater than 70 which correspond to rough bed flows according to Graf and Altinakar (1998).

In Figure 11 the Reynolds stress profiles used for shear stress evaluation are presented. These values have been normalized with the shear velocity obtained from Reynolds stress method. From the same figure it is possible to see that for the three first conditions (S1.3C1 to S1.3C3), corresponding to lower flowrate values, the Reynolds stress distribution follows equation (10) but that does not occur for the remaining conditions.

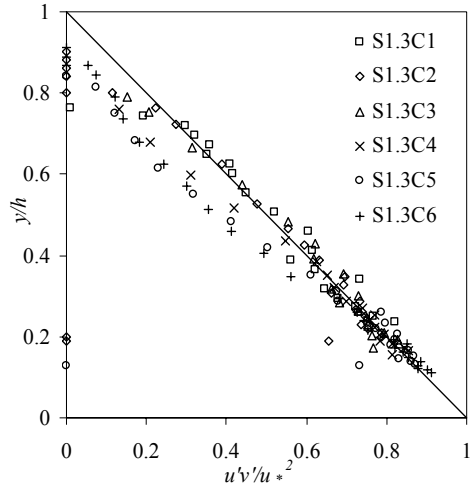


Figure 11. Shear stress values normalized with $u_*^2$.

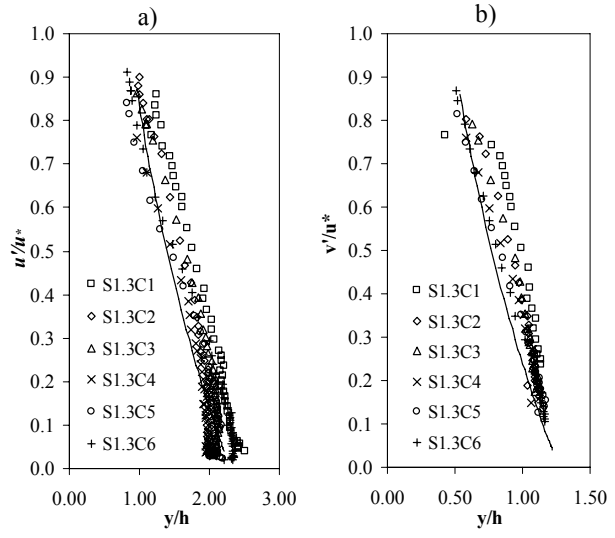


Figure 12. Vertical distribution of turbulence intensities components: a) longitudinal and b) vertical.

In order to check the obtained shear velocity values, namely the ones obtained through the Reynolds stress method, the measured normalized turbulence intensities profile are depicted in Figure 12 and compared with the corresponding empirical relationships (Nezu & Nakagawa (1993)):

$$\frac{u'}{u_*} = 2.30 \exp\left(-\frac{y}{h}\right) \tag{15}$$

$$\frac{v'}{u_*} = 1.27 \exp\left(-\frac{y}{h}\right) \tag{16}$$

where $u'$ = longitudinal turbulence intensity and $v'$ vertical turbulence intensity.

It is possible to see from the experimental results that Nezu and Nakagawa (1993) figured equations (15) and (16) are a good approximation in supercritical rough turbulent flows.

### 4.2.3 *Friction Factor Values Comparison*

The friction factor, λ, can be written as (Graf & Altinakar (1998)):

$$\sqrt{\frac{8}{\lambda}} = \frac{U}{u*} \tag{17}$$

where $\lambda$ = friction factor and $U$ = mean velocity.

For smooth flows the friction factor can be determined by the Prandtl-von Kármán equation for smooth flows (Chow (1959)):

$$\frac{1}{\sqrt{\lambda}} = 2\log\left(\mathrm{Re}\sqrt{\lambda}\right) + 0.4 \tag{18}$$

where $\lambda$ = friction factor.

And for rough channel flows the following relationship is valid (Chow (1959)):

$$\frac{1}{\sqrt{\lambda}} = 2.21 + 2.03\log\left(\frac{R_h}{k_S}\right) \tag{19}$$

Equation (18) and (19) are plotted in the Moody diagram, Figure 13, along with the obtained experimental data from this and previous studies.

The results for perspex and sandpaper depicted in Figure 13 show, as expected for smooth beds, that equation (18) is suitable to describe the measured frictions factors. When considering bed of uniform glass spheres it is possible to see that friction factor values are shifted into a parallel line to the one representing equation (18) which corresponds to equation (19) for different equivalent roughness, $k_S$. As shown in the same figure the consideration of a $k_S$ value equal to the spheres diameter equation (19) fits the experimental data obtained through the application of the Log-Law method. For a $k_S$ value of haft the diameter of the spheres the referred equation lead to a better approach to the experimental values obtained using the Reynolds stress method.

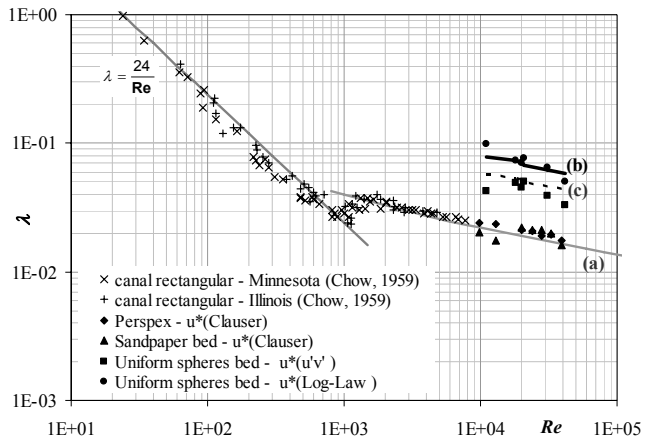


Figure 13. Experimental obtained friction values (with the method used to calculate the corresponding shear stress values in parenthesis) represented in comparison with the literature: (a) equation (18); (b) equation (19) with $k_S=D$; (c) equation (19) with $k_S=D/2$. (Adapted from Chow (1959)).

It must be pointed out that, taking into account the considered Reynolds number range and the usual criteria classification based on the roughness Reynolds number, the studied flows would be expected to be on a turbulent rough flow regime, to which a constant friction factor should correspond, although that is not verified.

## 5 CONCLUSIONS

In this paper different methods to determine the shear stress were used on flows characterized by high Reynolds and Froude numbers. A direct method provided by a Doppler shear stress probe proved to be an efficient and practical way to evaluate the shear stress. Its major disadvantage is the fact that the probe's volume control must be inside the viscous sub-layer which limits its application to smooth walls. Since it was not possible to use the shear stress probe for rough beds, different indirect methods were used and compared. It was possible to confirm that one of the methods, the Log-Law based one, led to shear stress values quite different from the ones obtained through the other methods, enabling to confirm the idea that maybe it is not suited for rough bottom channel flow conditions.

The shear velocity values obtained by the total stress method were similar to the ones obtained from the Reynolds stress method apparently and naturally because the form-induced stress have not shown considerable magnitude for the study conditions However, we shall emphasize that it was not possible to measure below the crests of the spheres, and that could eventually have led to observe some major differences. In fact, anyway, due to the uniformity of the bed a constant value of the displacement height was obtained for all tested flow conditions, which is in the line of the literature indications.

It was also possible to verify that, for the considered type of flows (high Reynolds and high Froude numbers), the non-dimensional normal stress follow the same theoretical laws presented by Nezu & Nakagawa (1993) for smooth beds.

The comparison with the friction factor, λ, showed that the measurements carried out for the smooth bed fall over the corresponding theoretical curve, as expected. For the bed of uniform spheres it was possible to see that the values calculated with the Log-Law and the Reynolds stress methods fit well equation (19), adequate for turbulent flows on rough bed channels, considering equivalent roughness values equal, respectively, to the spheres' diameter and to half the spheres diameter.

Further studies of the best fitting criteria for the corresponding friction factor values must be carried out.

## ACKNOWLEDGMENTS

This work was sponsored by PhD scholarship ref. SFRH/BD/19575/2004 from Fundação para a Ciência e a Tecnologia, Portugal.

## REFERENCES

Acharya, M., Bornstein, J., Escudier, M. P., Vokurka, V. 1985. Development of a Floating Element for the Measurement of Surface Shear Stress. AIAA Journal, 23(3), 410-415.

Bayazit, M. 1976. Free Surface Flow in a Channel of Large Relative Roughness, Journal of Hydraulic Research, 14(2), 115-125.

Biron, P. M., Robson, C., Lapointe, M. F., and Gaskin, S. J. 2004. Comparing different methods of bed shear stress estimates in simple and complex flow fields. Earth Surface Processes and Landforms, 29, 1403-1415

Chow, V. T. 1959. Open-Channel Hydraulics. MacGraw-Hill International Editors.

Durst, F., Melling, A., Whitelaw, J.H. 1981. Principles and Practice of Laser-Doppler Anemometry. Academic Press, London, 2nd edition, 1981

Ferreira, R., Franca, M., Leal, J. 2008. Flow Resistance in Open-Channel Flows with Mobile Hydraulically Rough Beds. River Flow 2008. 1, 385-393.

Gharib, M., Modarress, D., Fourguette, D., Wilson, D. 2001. Optical Microsensors for Fluid Flow Diagnostics. American Institute of Aeronautics ans Astronautics, Inc.

Graf, W. H., Altinakar, M. S. 1998. Fluvial Hydraulics. Wiley.

Grass, A. J. 1971. Structural features of turbulent flow over smooth and rough boundaries, Journal of Fluid Mechanics, 50(2), 233-255.

Pokrajac, D., Finnigan, J. J., Manes, C., McEwan, I., Nikora, V. 2006. On the definition of the shear velocity in rough bed open channel flows. RiverFlow. Taylor & Francis Group, 1, 89-98.

Nezu, I. Nakagawa, H. 1993. Turbulence in Open-Channel Flows. A. A. Balkema
Rowinski, P. M., Aberle, J., and Mazurczyk, A. 2005. Shear velocity estimation in hydraulic research. Acta Geophysica Polonica, 53(4), 567-583
Tavoularis, S. 2005. Measurement in fluid Mechanics. Cambridge University Press.
Tennekes, H., Lumley, J.L., 1972. A First Course in Turbulence. The MIT Press, Cambridge
Young, A. D. 1989. Boundary Layers. Oxford – BSP Professional Books.